Robust event-based non-intrusive appliance recognition using multi-scale wavelet packet tree and ensemble bagging tree

Yassine Himeur[a,*], Abdullah Alsalemi[a], Faycal Bensaali[a], Abbes Amira[b]

[a] *Department of Electrical Engineering, Qatar University, Doha, Qatar*
[b] *Institute of Artificial Intelligence, De Montfort University, Leicester, United Kingdom*

HIGHLIGHTS

- An event-based non-intrusive appliance recognition.
- A multi-scale wavelet packet tree descriptor for feature extraction.
- Appliance classification using ensemble bagging tree.
- A robust non-intrusive load monitoring for energy efficiency.
- A frequency-based event detection for non-intrusive load monitoring.

ARTICLE INFO

ABSTRACT

Providing the user with appliance-level consumption data is the core of each energy efficiency system. To that end, non-intrusive load monitoring is employed for extracting appliance specific consumption data at a low cost without the need of installing separate submeters for each electrical device. In this context, we propose in this paper a novel non-intrusive appliance recognition system based on (i) detecting events in the aggregated power signal using a novel and powerful scheme, (ii) applying multiscale wavelet packet tree to collect comprehensive energy consumption features, and (iii) adopting an ensemble bagging tree classifier along with comparing its performance with various machine learning schemes. Moreover, to validate the proposed model, an empirical investigation is conducted on two real and public energy consumption datasets, namely, the GREEND and REDD, in which consumption readings are collected at low-frequencies. In addition, a comprehensive review of recent non-intrusive load monitoring approaches has been conducted and presented, in which their characteristics, performances and limitations are described. The proposed non-intrusive load monitoring system shows a high appliance recognition performance in terms of the accuracy, F1 score and low time complexity when it has been applied to different households from the GREEND and REDD repositories, in which every house includes various domestic appliances. Obtained results have described, e.g., that average accuracies of 97.01% and 96.36% have been reached on the GREEND and REDD datasets, respectively, which outperformed almost existing solutions considered in this framework.

1. Introduction

Energy efficiency is considered as a demanding research topic and more attention is paid to it recently due to the benefits that can bring to the environment and society [1]. Recent studies have been reported that the best method to achieve higher energy savings in households is through monitoring each home appliance separately. However, this can be very costly, especially when using separate plug power meters for each domestic appliance [2,3]. In this regard, the best alternative solution is to use non-intrusive load monitoring (NILM) procedures that can separate aggregated power signal of a household or other buildings into the consumption of each specific appliance independently [4]. This is can be a very fruitful strategy due to the fact that providing individual power consumption of each appliance cannot only incentivize consumers to use less electrical power [5], however, it further supplies them with indicators about practical know-how and even more offers

specific perceptions of the context and activities of end-users [6,7].

Furthermore, NILM techniques are generally divided into two main categories of non-event-based and event-based [8]. The former, it is mainly devoted on the use of statistical models, while the latter, which is the purpose of this framework, focalizes on three main challenges aiming at [9]: (1) detecting events and transition changes, (2) extracting a set of characteristics to efficiently discriminate between various devices and capture unique properties of each one in regard to the use context, given that every group of devices has its specific electrical consumption signature, environment and use scenario (e.g. house, academic building, factory, etc.) [10]; and (3) selecting the appropriate learning architecture to classify appliances based on the extracted features [11]. Overall, both categories have the same final purpose that aims at splitting an aggregate energy consumption signal into multiple fine-grained energy records and thereby recognizing the appliance category of each individual fingerprint [12].

In consequence, the appliance recognition or identification task is an essential step in the NILM system. Consequently, performing a device recognition through the electrical network results in an automatic identification of each appliance from its power consumption signal [13]. Further, it leads also into collecting fine-grained consumption signatures of domestic electrical devices (such as air conditioner, TV, fridge, coffee machine, dishwasher, etc.) [14]. Hence, they are a stepping-stone into decreasing power usage and promoting energy efficiency through providing the user with consumption statistics of each appliance [15]. Moreover, the appliance identification task allows other important applications, among them the identification of energy hungry devices [16], determination of suspicious electricity consumers [17], fault and anomaly detection [18,19], occupancy detection [20,21], detection of suspicious or unidentified appliances and eventually helps in developing reliable energy disaggregation systems [22,20].

To that end, in this paper, we propose a novel NILM architecture based on the following contributions: (1) a powerful event detection scheme is introduced, which works in the frequency-domain and deploys a filtering process in the Cesptrum space to reduce the noise generated by the electrical devices, resulting then in a better detection of transitional changes occurred in the power signals; (2) an efficient feature extraction approach is introduced that is based on the multiscale wavelet packet tree (MSWPT). It is worth noting that, to the best of our knowledge, this is the first framework that discusses the use of MSWPT for NILM purpose. The MSWPT is a good candidate for analyzing stationary and even non-stationary signals. This is because the multiscale time frequency examination provides a large dimensional quantity of data and thereby supplying more details on the detected events and capturing the peculiarities of every appliance through removing irrelevant noise frequencies; and (3) an ensemble bagging tree classifier (EBT) is introduced, which is designed to efficiently classify appliances based on the features extracted from the detected events. The use of the MSWPT is validated using a comprehensive comparison with reference to several machine learning algorithms. In addition, an extensive survey of existing NILM techniques has been conducted and presented, in which their properties, performances and drawbacks are seized. Following, a profound performance investigation is managed using two large-scale and realistic databases, entitled the GREEND [23] and REDD [24] datasets. The former contains daily load profiles of more than 30 appliances groups, which are collected from six different houses. Each device is monitored for a long period ranging from 4 to 12 months. However, the latter contains consumption fingerprints of more than 20 appliance classes gathered at a resolution of 1/3 Hz.

In addition, the possibility of developing the proposed NILM system as an industrial application is assessed, where the time complexity of proposed system versus other MSWPT-based machine learning solutions has also been investigated. Further, validating the proposed NILM system on the GREEND and REDD datasets, in which the consumption data are gathered at low frequency (1 Hz and 1/3 Hz, respectively), has two main advantages; first, it can economize the power usage and data

storage without hindering the recognition task. Second, good recognition performances are achieved in terms of various benchmarking metrics at a low computational complexity.

The rest of this paper is structured as follows. Section 2 presents various recent schemes pertaining to the two main categories of NILM systems that are event-based and non-event-based. A comparison is performed between techniques belonging to both groups, their limitations and drawbacks are highlighted as well. Section 3, explains the steps required to implement the proposed NILM system, in which thorough explanations have been presented about the proposed event detection scheme, MSWPT-based feature extraction approach and ensemble bagging tree classifier. After that, a deep performance investigation carried out in accordance to various metrics is presented in Section 4 on both the GREEND and REDD datasets. Finally, conclusions on the appliance recognition study investigated in this paper are drawn in Section 5 on the basis of the output analysis and therefore the principal orientations for future works are identified as well.

2. Related works

Overall, NILM systems could be divided into two main categories of non-event-based and event-based. The first, focuses on methods that are not dependent on training in a specific building and could separate energy traces of individual appliances from the aggregate load [25]. One of the methods that have been commonly investigated in this domain is the use of statistical models such as Hidden Markov Models (HMMs), probabilistic models and higher-order statistics (HOS). The second, refers to techniques that identify changes in the appliance state by using event detection, classification, and then an approach for calculating energy consumption for individual appliances [26].

2.1. Non-event-based NILM schemes

This class is mainly based on the use of statistical models, including HMMs, probabilistic models and HOSs to segregate the aggregated power signals into appliance-level data. In fact, the NILM issue represents a time dependent problem in which statistical models are greatly targeted as a suitable solution. Recently, HMMs-based methods have been receiving increasing attention. Various NILM techniques, adopting the HMMs as the central part of their architecture, have been proposed in the literature.

In [27], a hierarchical method that can model various devices within the same category using a Bayesian consideration of HMMs is proposed. A specific device consumption model is then generated through the combination of the various HMMs settings. In this regard, a completely new device model is designed to represent an appliance class form 3 to 6 device examples. In [28], a HMMs-based classification is implemented on temporal power consumption sequences to segregate aggregated load profiles. It aims at (i) detecting device states at a low resolution and (ii) adopting these features to model appliance categories and classifying candidate devices. In [29], Makonin et al. propose an energy segregating technique based on the use of a super-state HMMs and Viterbi model, hence allowing a better reliance between appliance signatures and an easy disaggregation of multi-state energy consumptions. The Viterbi scheme is used to effectively estimate the sparse arrays used to perform the NILM task.

The problem of energy disaggregation is solved based on the rollout of the Viterbi decoding process by Kong et al. [30]. This decoding is particularly deployed to predict the probable sequences of the hidden conditions of HMMs in regard to the observation sequences. In [31], virtual stochastic sensors and hidden non-Markovian models (HnMM) are employed to abstract electrical device signatures while considering the precise period of switching on every device. In [32], the NILM problem is solved using HOS, which are implemented on separate appliance energy consumption signals. In [33], power consumption patterns of each electrical device are identified based on estimating the

probability of events occurred for a set of electrical devices using a mixture of Bernoulli distributions. In [34], the additive factorial approximate maximum a posteriori (AFAMAP) is used to extract power signatures from electrical devices using recursive fuzzy c-Means and HMMs.

In [35], two ML models based on unsupervised occurrence based detection and Markov chain device energy consumption modeling are combined in order to implement an NILM framework. The latter enables a fast and on-line domestic device identification using consumption patterns. In [36], a combination of NILM and load profiling process is implemented to collect appliance-level consumption fingerprints at a low sampling rate of 15 min. This technique focuses on using the HMMs algorithm to model consumer behavior, extracting load usage profiles and statistical patterns adequately and finally generating device-level consumption footprints.

In [37], an additive factorial HMMs is deployed to develop an NILM solution based on the combination of active/reactive power data. In this context, a bivariate HMMs is used to model each device consumption model while the emitting signatures are simply the combination of active/reactive power usage. In [38], a fusion of the factorial HMMs and recurrent sub-sequence dynamic time warping (SDTW) is operated to design an NILM with a low complexity. The factorial HMMs are used to extract the preliminary representation of consumption trajectories while the recurrent SDTW is deployed to classify the appliances based on a distance estimation. In [39], the difference factorial HMMs (DFHMMs) along with the Kronecker process are used to develop an NILM system that can retrieve appliance-level consumption patterns, especially in the case of electric space heaters (ESH). This framework has a good robustness to noise generated by other unknown appliances. In [40], active power records are utilized to model domestic electrical devices as factorial HMMs. In addition, an aggregated-consumption modeling approach is introduced. Time windows are then investigated using the probabilistic computing to capture correct parameter settings that help in achieving the power disaggregation.

In [41], an NILM framework based on factor HMMs is introduced where the devices' current records are considered as the power consumption features. A statistical model is then established to fit the aggregated current and specific currents of multiple devices. Following, a factor HMMs based approach is used to capture operation states of every electrical device that help segregating the aggregated load. In [42], HOSs pulled from current signals are used to model electrical appliance signatures.

Table 1 presents a comprehensive comparison between different statistical models according to different parameters, including the adopted architecture, number of monitored appliances, frequency resolution and achieved accuracy.

2.2. Event-based NILM schemes

This type of methods is mainly categorized based on two important modules participating in their development, the feature extraction process and learning models. Traditional categories of NILM systems are mainly focusing on the extraction of steady-states and transient-states based characteristics and on the use of traditional machine learning (ML) algorithms. However, new techniques have been proposed recently relying on other new trends of power signal analysis. This category of schemes is considered as non-conventional NILM systems.

2.3. Feature extraction

To categorize recent feature extraction schemes, three main classes are highlighted as follows:

a. Graph signal processing (GSP) features: GSP is a popular research topic that aims at representing the stochastic properties of signals using graphs. In [59], an event-based graph scheme is proposed to design signatures of power consumption signals and also to minimize the training time and reduce computational complexity of traditional graph-based approaches. In [60], different graph-based multi-label approaches are introduced for identifying electrical appliances with a semi-automatic manner. In [61], the NILM performance is improved using a generic GSP-based scheme that relies on applying graph-based filters, which can help in detecting on/off occurrences through mitigating the noise generated from electrical appliances.

b. Time-frequency analysis: this kind of analysis is among the well-know methods conducted to extract features in many other research fields. In the case of NILM, it can be used to solve the overlapping issue and provide more resolution about the power consumption footprints. In [62], time-frequency signatures are captured using a multiresolution S-transform. In [63], wavelet analysis is performed, followed by a power spectrum extraction from the wavelet coefficients based on the Parseval's theorem, while in [64] the energy of wavelet patterns at multiple decomposition levels is used to represent appliances. Welikala et al. [65] use a recursive deployment of the Karhunen-Loeve process to collect a robust and fine-grained spectrum. Moreover, disaggregation of power consumption footprints is realized using deconvolution approach. In [66], two classification techniques, namely RAkEL and MLkNN, experiencing time and wavelet domain analysis, are used to collect power characteristics. In [67], a time-related non-event-based technique is proposed to detect if an appliance is on mode switch on through using a sliding window and thus extracting unique signature for each device. In [68], two TD feature bags are picked up using the nonactive-current wave and the voltage-nonactive current shape. In

Table 1
An overview of the existing NILM systems based on statistical models.

Work	Category	Sub-category	Architecture	# appliances	Resolution (Hz)	Accuracy (in %)
[27]	unsupervised	HMMs	Bayesian HMMs	5	1–1/8	N/A
[28]	un-supervised	HMMs	temporal sequence + HMMs	N/A	1/600	75.25
[29]	supervised	HMMs	super-state HMMs + Viterbi model	6	1/60	94.86
[30]	supervised	HOSs	ANN + 2nd and 4th order statistics	11	15.36	97
[31]	supervised	HnMMs	virtual stochastic sensors (VSS)	11	12 k	94
[32]	un-supervised	HMMs	iterative k-Means	N/A	1/3	85
[33]	un-supervised	Probabilistic	Bernoulli distributions	N/A	1	80
[34]	un-supervised	AFAMAP	recursive fuzzy c-Means + HMMs	6	1/600	79
[35]	un-supervised	HMMs	Markov chain + mean-shift clustering	5	1/6	74.4
[36]	un-supervised	HMMs	activity Markov chain	8	1/900	N/A
[37]	un-supervised	HMMs	additive Factorial HMMs	5	1/60	76.76
[38]	semi-supervised	HMMs	factorial HMMs + recurrent SDTW + SDTW	11	1/60	61
[40]	un-supervised	HMMs	factorial HMMs	6	1/120	N/A
[39]	un-supervised	HMMs	difference factorial HMMs	N/A	1	95
[41]	un-supervised	HMMs	variant of factor HMMs	7	N/A	92.78
[42]	supervised	HMMs	viterbi decoding + HMMs	12	1/3	96

Table 2
An overview of the existing NILM systems based on deep neural networks.

Work	Category	Sub-category	Architecture	# appliances	Resolution (Hz)	Accuracy in (%)
[43]	supervised	RNN	LSTM	18/9	1	N/A
[44]	supervised	Gated CNN	gated linear unit (GLU)	6	1/3	N/A
[45]	supervised	CNN	ReLu + variational autoencoder	6	1/6	N/A
[46]	supervised	CNN	CNN with gradient descent	11/15	30, 44 k	77.6/75.4
[47]	supervised	CNN	denoising autoencoder	5	1/3, 1/6, 1/60	N/A
[48]	supervised	CNN	elliptical Fourier features	12	30 k	80.4
[49]	semi-supervised	CNN	BiLSTM + temporal ensembling CNN	4	1/3	97.45
[50]	supervised	CNN	background filtering	4	1/6	96.92
[51]	supervised	Causal CNN	1D CNN + dilated causal layers	20	1/60	94.7
[52]	supervised	CNN	ResNet + DCRN	5	1/6	96.67
[53]	supervised	CNN	CNN with Differential Input	3	1	N/A
[54]	supervised	CNN	CNN with residual unit	21	4 k	97.9
[55]	supervised	CNN	scale- and context-aware network	3	1/3	83
[56]	supervised	CNN	ReLu + data augmentation/pre-processing	2	N/A	76.83
[57]	supervised	CNN	siamese neural networks	11/15	30, 44 k	90/85
[58]	supervised	CNN + RNN	ReLu + GRU	4	1/3, 1/6	76/82

[69], a two-step feature collection approach is proposed where candidate events are firstly selected, then a filtering process is performed at TD to extract power fingerprints. In [8], a linear time-invariant method is proposed to describe aggregated on/off events of each device. In [70], a spatio-temporal analysis is conducted to retrieve multivariate time-series characteristics of load usage. In [71], an empirical mode decomposition (EMD) based feature extraction scheme is proposed. After obtaining the intrinsic mode functions (IMFs) patterns using the EMD, the pertinent features are extracted via analyzing their time-frequency space. In [72], shapelet features are extracted from time-series current envelopes, which are already determined from initial current trajectories through capturing and connecting peak points of every sample. In addition to the aforementioned works, a statistical feature extraction technique for normalized current data is proposed in [73]. Supervised classifiers are then applied to detect each appliance class. In [74], Jimenez et al. propose an NILM system using the S-Transform to extract appliance features that are then fed into an SVM classifier to recognize each electrical device. The performance of the S-Transform has been compared to a wavelet packet tree (WPT), in which only 3 level of decompositions are used. however, this is not sufficient to extract pertinent appliance features. However, in this framework, the proposed MSWPT is used using 7 level of decomposition and a feature selection in each sub-band to construct the final feature vector. This leads to a better performance in terms of the accuracy and F-score.

2.4. Deep neural network (DNNs)

One of the popular and recent learning solution focuses on the use of deep neural networks (DNNs). Three main architectures are mostly investigated in the state-of-the-art, deep convolutional neural network (CNN), recurrent neural networks (RNN) and denoising autoencoder (dAE). In addition, various variants of these architectures are proposed as well.

Learning models can also be classified based on the nature of the training process required for their implementation, and hence it can be either supervised or unsupervised. Although the supervised models are the most targeted techniques, unsupervised solutions have also attracted a growing attention because the training of NILM frameworks is usually avoided. Thus, unsupervised learning models require less effort from the end-user compared to the supervised solutions [75].

In [27,28], conventional CNN-based architectures with various kernels is proposed to solve the NILM problem. Mauch et Yang [30] propose a supervised NILM technique based on a deep recurrent long short-term memory (LSTM) network. In [31], a CNN with gradient descent architecture is used to train voltage-current (V-I) trajectories and classify appliances in an NILM system. In [44], a gated CNN is

introduced to segregate aggregated power signals. Specifically, the gated-linear-unit (GLU) was deployed in convolutional layers for classifying the activations of target devices in each time interval. In [55], to address the context dependencies of load usage footprints, Chen et al. design an improved CNN architecture on a scale-and-context-aware network, which helps enhance the disaggregation accuracy in comparison with traditional CNN. In [56], a deep CNN architecture based on the rectified linear units (ReLU) with a data augmentation and preprocessing approach is proposed to disaggregate electricity consumption signals. Authors in [58], proposed an NILM system based on CNN and gated recurrent unit (GRU) with the object of classifying appliances' states and estimating power consumption. A semi-supervised multi-label CNN system was introduced in [49] to draw high-level power consumption fingerprints using bidirectional LSTM (BiLSTM).

In [45], an NILM system is implemented using a CNN based variational autoencoder (VAE) with the ReLU as the activation function. In [50], synthetic aggregated patterns were used to train a CNN algorithm based on AlexNet architecture, then background filtering was also introduced to generate data to further train the CNN to collect appliance-level footprints. In [51], a causal 1D CNN based on wavelet and neural networks (WaveNet) architecture is presented to reduce the complexity and achieve a better energy disaggregation performance. In [48], a CNN is trained using elliptical Fourier features of devices' V-I trajectories that are represented as images. In [52], a CNN based NILM system was developed using a dilated-convolution residual network (DCRN). The latter is used with a view of facilitating the network-optimization task and further solving the vanishing gradient issue. In [76], the authors train a group of autoassociative neural networks (AANNs) in the way that every network is adjusted using the features of a specific household device. After that, the AANNs are implemented in parallel architecture where a candidate device can be recognized through making a competition between the AANNs in which the closest identification is approved. In [47], the NILM process was considered as a noise mitigation issue and a denoising autoencoder structure was deployed. Specifically, the authors attempted to reconstruct disaggregated signals (appliance-level data) from their aggregated representation (considered as the noisy signal).

Table 2 summarizes the characteristics of the aforementioned DNNs-based NILM systems and specifies a useful comparison in terms of their accuracy performances and other relevant parameters such as the adopted architecture, number of monitored appliances and frequency resolution.

Although the presented DNNs-based NILM architectures have been deeply investigated in the literature, they still suffer from several drawbacks and limitations that (i) hinder developing robust NILM systems, (ii) make it difficult to implement real-time solutions and

further most of them have not yet been overcome. Moreover, one of the main drawbacks of DNNs is their high computational complexity, which makes it difficult to implement real-time NILM systems based on these algorithms.

For non-event NILM models, although they can be considered as a promising concurrent solution to event-based techniques, their major limitation is related to the fact that most of them still have a low identification performance, in which most of them have an accuracy below 90%. Therefore, these approaches still need deep investigations in order to improve their accuracy. Further, since they rely mainly on complex probabilistic estimation and prediction, their implementation on embedded systems is difficult, even impossible. From another side, it is worth noting that in most of existing NILM frameworks, large-scale datasets with different sampling rates are adopted with selective specific houses, devices and time periods, making empirical performance outputs very difficult to reproduce.

3. Proposed system

Under this section, an elaborate description of the proposed NILM is presented. The main steps used to develop the proposed architecture are explained in the following sub-sections, including data pre-processing, event detection, feature extraction based on a MSWPT descriptor and appliance classification using an EBT classifier. The block diagram of the proposed NILM system is depicted in Fig. 1.

3.1. Data pre-processing

The raw data collected from the GREEND and REDD experimental campaigns are incomplete and they cannot be fed to the event-detection and feature extraction modules directly without preliminary processing. Consequently, it may be required to clean the data through checking for missing observations (NaN samples) and thus replacing them by zeros. Moreover, up to 80000 samples are recorded from daily energy consumption of each electrical device. A re-sampling process is performed in all power consumption signatures and thereby fingerprints with a length of 30000 patterns are then used under this framework.

3.2. Event detection

Event detection contributes significantly in developing a robust NILM system because it aims at accurately detecting state-transitions of electrical devices (events) from aggregated power signals collected in household environments.

In this framework, the event detection task is performed using a simple yet effective technique, which works in the frequency-domain and uses a Cepstrum filtering to suppress the noise that can hinder detecting transition changes effectively. The main advantage of this scheme is that no additional information about electrical devices is needed, and further nor training tests are required. The event detection steps are summarized in Algorithm 1 and Fig. 2.

Algorithm 1. The event detection algorithm used in the proposed NILM system.

Result: Ω_k: events detected from the aggregated power consumption signal

a. Divide the aggregated power signal $s(i)$ into M windows $w^m(i)$, where $m = 1, 2, \cdots, M$; **while** $m \leq M$ **do**

    1. Transform the window $w^m = \{s_i, s_{i+1}, ..., s_{i+n}\}$ to the frequency-domain via the Fourier transform

$$W^m[k] = \sum_{j=1}^{n} w^m[j] e^{-2\pi i k j/n}, \qquad 0 \leq k \leq n \tag{1}$$

    2. Convert the obtained frequency information to the quefrency domain as

$$q^m[n] = \frac{1}{N} \sum_{k=0}^{N-1} \log_{10}(|W^m[k]|) e^{2\pi i n k/N}, \qquad 0 \leq n \leq N \tag{2}$$

    3. Smooth the Cepstrum components using a filter F. Following, transform them back to frequency domain using the Fourier transform

$$\widehat{W^m}[k] = \sum_{j=1}^{n} F[j] q^m[j] e^{-2\pi i k j/n}, \qquad 0 \leq k \leq n \tag{3}$$

    where

$$F[j] = 1 - 0.5(1 - \cos(2\pi j/n)), \qquad 0 \leq j \leq n \tag{4}$$

    This leads to the suppression of all the components except the very low and high frequencies, which correspond to steady-state and step change in the time-domain, respectively.

    4. Convert the frequency components to a decibel (dB) space

$$\widehat{W}_{dB}^m[k] = 20 \log_{10}(\widehat{W^m}[k]) \tag{5}$$

    5. Detect if an event is present by checking the frequency components as follows:

$$\Omega^m[k] = \begin{cases} 1 & \text{if } \min(\widehat{W}_{dB}[k]) > \tau \\ 0 & \text{else} \end{cases} \tag{6}$$
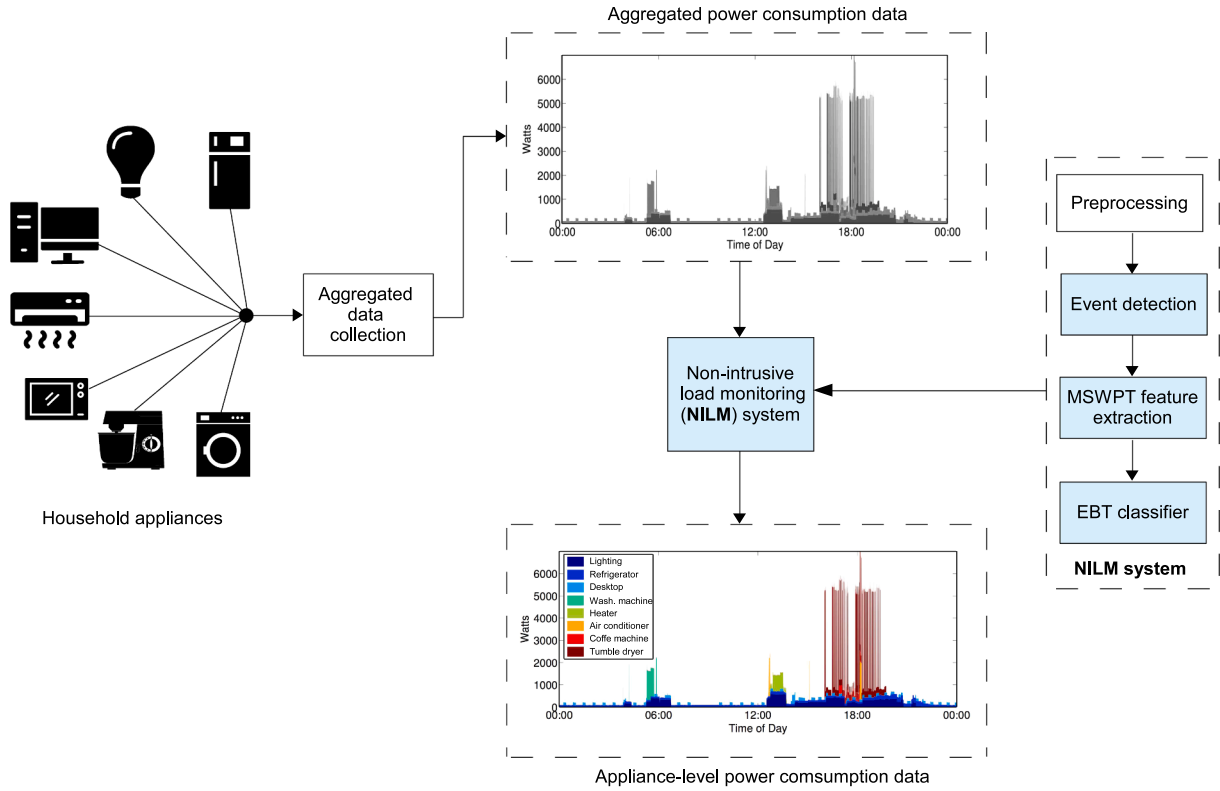
end

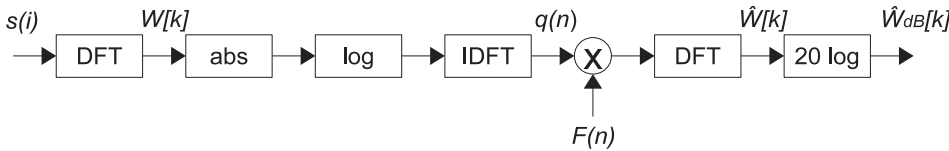**Fig. 1.** Flowchart of the proposed appliance recognition system based on MSWPT and EBT.

Fig. 2. Flowchart of the event detection scheme.

3.3. Feature extraction using multi-scale Wavelet Packet Tree

In order to recognize the events detected in the previous step, a powerful feature extraction should be used that can easily discriminate between different events pertaining to different appliance classes, and on the other hand helps correlate between events pertaining to the same appliance categories. Multi-scale analysis of the MSWPT is regarded pertinent for exploring and extracting features from similar signals. It manifests proper frequency resolution as well as a finite temporal resolution, and thereby it can easily retrieve low frequency elements (approximation) and specify high frequency samples (detail). Further, the MSWPT is implemented through disseminating the liaison among the multi-resolution approximations and wavelet filters.

Using the MSWPT, the event space Ω extracted using the Algorithm 1 from each electrical power signal is split into lower frequency coefficients L_{j+1} (approximation) and high frequency coefficients H_{j+1} (details). Where i is the decomposition level (scale resolution) and j is the index of the sub-band. The splitting process is realized by breaking up the orthogonal base $\{\phi_i(t - 2^iJ)\}_{i \in Z}$ of $\Omega_{i,j}$ (where $\Omega - 0, 0$ is the initial event space) into two novel orthogonal bases $\{\phi_{i+1}(t - 2^{i+1}J)\}_{i \in Z}$ of $\Omega_{i+1,2j}$ and $\{\varphi_{i+1}(t - 2^{i+1}J)\}_{i \in Z}$ of $\Omega_{i+1,2j+1}$, while $\phi()$ is the function used for resizing and $\varphi()$ represents the wavelet filters, they are given as

$$\phi_{i,j}(t) = \frac{1}{\sqrt{|2^i|}}\phi\left(\frac{t - 2^iJ}{2^i}\right) \tag{7}$$

$$\varphi_{i,j}(t) = \frac{1}{\sqrt{|2^i|}}\varphi\left(\frac{t - 2^iJ}{2^i}\right) \tag{8}$$

It is worth noting that the parameter 2^i represents the resizing criteria and it defines the rate of compression or resizing.

The main difference between MSWPT and conventional wavelets is that MSWPT splits the low frequency samples as well as the high frequency coefficients using a quadrature mirror filter (QMF) bank. The operation is then restarted I times, with $I \leqslant \log_2 N$, and N represents the length of the original event. Consequently, $I \times N$ observations are obtained. Therefore, at decomposition state i ($i = 1, 2, ..., I$), the tree produces $N/2^i$ observations. This recursive splitting scheme creates the MSWPT structure, which is specified with various frequency localization properties. Fig. 3 depicts a three level splitting process using the MSWPT. When the desired scale i is reached, the pertinent features are finally extracted by combining the first half of samples from each band. Consequently, a feature vector G having half the length of the initial event vector $\Omega_{0,0}$ is constructed. After applying the MSWPT process to all appliance power signals in a specific dataset, the feature vectors extracted will be then used to train the EBT classifier in the next step.

3.4. Ensemble bagging tree classifier

A detailed description of the EBT algorithm used in under this framework is given in this section. EBT is a machine learning architecture where various weak learners are used in the training process to fix similar issue and then fused to obtain better prediction performance [77].

3.4.1. Bagging theory

For a classification problem, a prediction function $g(v, G)$ forecasts a class $c \in \{l, 2, 3, ..., C\}$
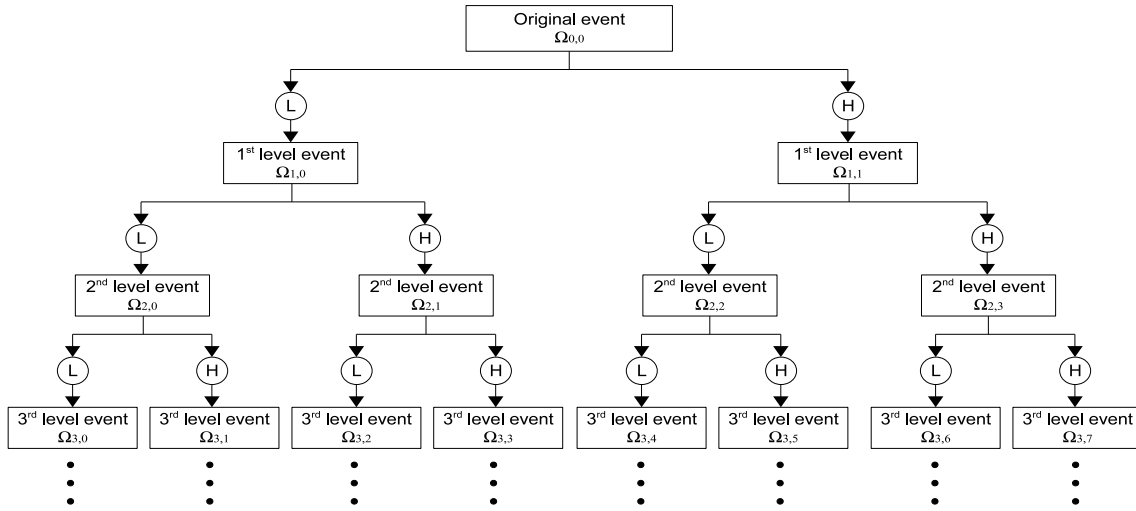
Fig. 3. Example of the MSWPT splitting of $\Omega_{0,0}$ into tree structured subspaces.

$$\Im(c|v) = P(g(v, G) = c) \qquad (9)$$

$\Im(c \mid x)$ can be interpreted as: for several independent duplicates of the learning group G, g forecasts the class tag j for the input v with proportional occurrence $\Im(c \mid v)$. Also, if $P(c/v)$ stands for the probability, the observation v triggers the class c. Afterward, the probability of properly classifying the produced event at v is

$$\sum_c \Im(c|v)P(c|v) \qquad (10)$$

and the total probability of accurate classification is estimated according to

$$T_C = \int \left[\sum_c \Im(c|v)P(c|v)\right] P_V(dv) \qquad (11)$$

where $P_V(dv)$ depicts the probability distribution of v. Also, by considering Eq. 10, it is worth to mention that for every $\Im(c \mid v)$, we have

$$\sum_c \Im(c|v)P(c|v) \leqslant \max_c P(c|v) \qquad (12)$$

and the equality is reached only if

$$\Im(c|v) = \begin{cases} 1 & \text{if } P(c|v) = \max_i P(i|v) \\ 0 & \text{else} \end{cases} \qquad (13)$$

Interpreting $\Im(c|v)$ means that the conditional probability under the predicted class can reach the global accuracy according to formula 11. The total probability of true classification is given as
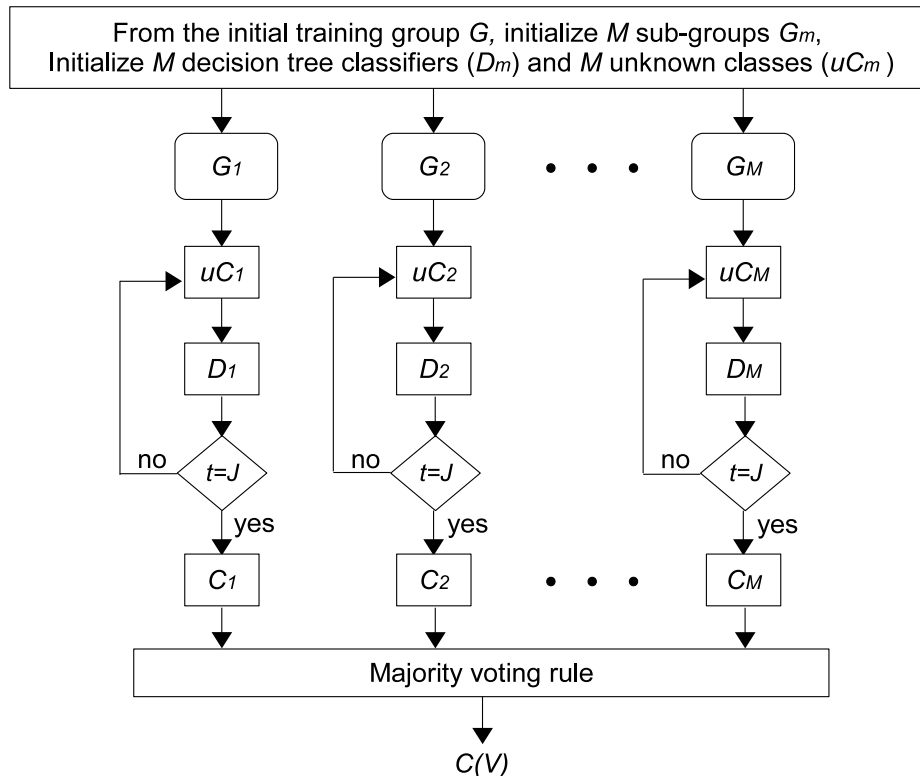

Fig. 4. Flowchart of the EBT Algorithm used to classify the appliances.

$$T_r = \int_{v \in S} \max_c P(c|v) P_v(v) + \int_{v \in S'} \left[\sum_c I(K_A(v) = c) P(c|v) \right] P_v(v) \tag{14}$$

where S represents the total set of input v where K is order-correct. As a consequence, if a classifier has good performance in the direction of being order-correct for almost all inputs v, accordingly the aggregation helps turn it into a roughly optimal classifier.

3.4.2. Ensemble bagging tree

In practice, the EBT is founded upon the bagging theory. Puts differently, it is based on extracting a large amount of variables from initial data samples, organizing them in various sets, and thus a specific technique is implemented to every bootstrap set. After that, a straightforward vote process for classification is used to fuse the outputs. Fig. 4 describes the implemented EBT algorithm.

Towards this regard, considering M sub-groups of the feature group G extracted using the MSWPT and M weak decision tree classifiers D_m, $m = 1, 2, ..., M$, and allowing the classifiers making J cycles of training. Every cycle group compounds an ensemble of primary training patterns, which are randomly drawn from training variables. Subsequent to primary training, variables appearing multiple times in each subset training cycle provide finally a succession of prediction functions $C_1, C_2, C_3, ..., C_M$. Therefore, the total prediction $C(V)$ has been just the fusion of these predictions using a voting process.

4. Experimental results

In order to help energy researchers and scientists testing their algorithms and solutions under realistic conditions, a set of publicly accessible databases has been proposed in the literature for different applications and using various sampling frequencies. As it can be found in literature, the datasets that are collected at low sampling rates are the most popular nowadays since they can economize the power usage and data storage even if they hinder the recognition task. However, in this study, we will prove that by handling the low sampling rate consumption patterns, the proposed solution can not only capture the most prominent features of each device, but also provides a high appliance recognition rate in addition to saving storage and power. To that end, two datasets, namely the GREEND and REDD are considered in this work to evaluate the proposed NILM system.

4.1. Evaluation metrics

The selection of criteria for evaluating an appliance recognition system is utmost importance given that this choice impacts the measure

Table 3
Description of the appliances monitored in each household.

Household	# appliances	Period (days)	Appliance description
0	6	242	Coffee machine, radio, fridge w/freezer, dishwasher, kitchen lamp, TV
1	3	474	Fridge, dishwasher, microwave
2	5	258	network attached storage (NAS), washing machine, drier, dishwasher, coffee machine
3	3	412	fridge w/o freezer, computer, TV
4	5	225	Total outlets, fridge w/freezer, electric oven, computer w/scanner and printer, washing machine
5	5	340	Lamp, stove, iron, LCD TV, fridge w/freezer
6	3	258	Plug 1 (Total ground and first floor), Plug 2 (total garden and shelter) and plug3 (total third floor)
7	6	138	TV w/decoder, fridge w/freezer, kitchen TV, ADSL modem, freezer, laptop w/scanner and printer

and comparison of the recognition scheme. The accuracy (acc) and F1 score are considered in this study. Further, the confusion matrix is considered as a simple yet efficient measure that may deserve to be inspected when treating a classification question. In fact, this factor provides a valuable synthesis of how good the classification architecture is performing. As such, it represents a useful and needful evaluation metric for any classification system. In addition, we have also used the normalized cross-correlation (NCC) for measuring the similarity of the raw events and MSWPT features extracted from the original events. The normalized correlation can be represented as the computation of the cosine of the angle θ among two signals (or feature vectors) x and y:

$$NCC = Cos(\theta) = \frac{x \cdot y}{|x||y|} = \frac{\sum_i x_i \cdot y_i}{\sqrt{\sum_i x_i} \sqrt{\sum_i y_i}}, \quad -1 \leqslant NCC \leqslant 1 \tag{15}$$

4.2. Dataset description

In the first stage of the evaluation, the GREEND [23] dataset is considered to investigate the performance of the proposed NILM system. The GREEND repository encompasses electricity consumption profiles (in Watts) measured at the appliance level during an experimental campaign implemented in 8 different households in Austria and Italy. This database is collected for a period ranging from 4 to 13 months at a sampling frequency of 1 Hz. The performance validation over this framework is managed using the six ensuing house configurations, which are selected randomly:

- Household 0: represents a separate domestic resident, including two floors in the region of Spittal an derDrau (Austria). This house was occupied by a retired couple that spent nearly all of their time on household labor.
- Household 1: describes an apartment dwelling containing only one floor in the region of Klagenfurt (Austria). It was inhabited by a couple, expending most of their time working, especially on weekdays, while at the weekends they were mainly being at the house.
- Household 2: is a separate residence villa containing two floors in the region of Spittal an derDrau (Austria). This home included three occupants, a husband that worked full time, a housewife and a 28 year old son that spent most of the time working.
- Household 4: represents a dwelling apartment containing two floors in Udine (Italy). This apartment was inhabited by a young working couple, passing almost of their time outside, they were just being indoors at nights and weekends.
- Household 5: describes an apartment dwelling a separate domestic resident encompassing two floors in Colloredo di Prato (Italy). This house was occupied by 3 persons; an employed husband, a housewife and an adult son that worked and spent most of the time outside.
- Household 7: stands for a separate villa incorporating two floors in the region of Basiliano (Italy). This resident was occupied by a retired couple that spent almost of their daylight time in the household.

Furthermore, each house contains a set of appliances that were observed for a period of more than four months and less than 13 months. The monitored appliances in each domestic building are reported in Table 3. As it can be shown, each household contains at least three different devices. Since the GREEND dataset includes appliance-level consumption fingerprints, the exaggerated signal is assumed to be the aggregation of energy consumed by the component appliances in each household as explained in [23,78]. In this regard, if N devices are considered in each house, and for every device the power signal at time t is described as $S_{i,t} = (s_{i,1}, s_{i,2}, ..., s_{i,T})$, where $s_{i,t} \in R+$. The aggregated power consumption is represented as $Z_t = \sum_{i=1}^{N} s_{i,t} + \varepsilon_t$,

Table 4
Impact of the threshold variation on the performance of the proposed event detection scheme.

| Threshold (τ) | GREEND | | | | | | REDD | | | | | |
	5	10	**15**	20	25	30	5	10	**15**	20	25	30
Home 1	96.13	97.59	**99.07**	98.31	97.67	97.01	97.36	97.96	**98.53**	98.14	97.6	97.01
Home 2	97.55	98.37	**99.42**	98.11	97.43	96.22	97.51	98.22	**98.68**	97.83	97.49	97.17
Home 3	96.25	97.14	**97.86**	96.88	96.38	95.77	95.95	96.76	**97.31**	96.88	96.10	95.64
Home 4	97.59	98.30	**98.73**	98.12	97.35	96.42	96.86	97.58	**98.20**	97.71	97.16	96.40

Table 5
Average performance of proposed event detection method with reference to other detectors.

| Dataset | GREEND | | | | | REDD | | | | |
Detector	χ^2	Sobel	On-ff pairing	Hybrid	Our	χ^2	Sobel	On-off pairing	Hybrid	Our
F-score (%)	98:06	87.89	97.07	98.81	98.93	97.17	83.42	96.23	97.75	98.01
Time (sec)	12.7	4.11	41.1	577.8	0.37	9.8	3.34	39.7	572.4	0.32

Table 6
Performance investigation of the proposed NILM system using the EBT classifier in comparison to various other machine learning algorithms.

| ML algo | Classifier parameters | house 0 | | house 1 | | house 2 | | house 3 | | house 4 | | house 5 | | house 6 | | house 7 | |
		acc	F1	acc	F1	acc	F1	acc	F1	acc	F1	acc	F1	acc	F1	acc	F1
SVM	Linear Kernel	92.6	90.76	48.28	30.43	88.53	88.24	92.3	91.43	91.39	89.67	90.41	89.33	90.51	89.62	85.39	84.86
SVM	Quadratic kernel	91.81	89.77	21.05	10.23	89.32	89.14	91.86	90.1	90.17	89.23	90.61	90.57	90.1	89.68	81.64	72.83
SVM	Gaussian kernel	92.63	90.95	76.52	65.63	88.21	88.24	92.08	91.37	88.63	75.94	90.24	89.81	88.64	93.3	79.32	70.24
KNN	K = 1, Euclidean dist	80.47	77.86	88.71	87.9	89.90	89.57	83.69	80.97	54.17	54.32	74.09	71.36	74.39	72.54	82.57	81.54
KNN	K = 10, Weighted Euclidean dist	69.38	65.2	70.34	65.98	87.16	86.02	76.28	74	91.49	74.7	71.9	66.78	73.49	71.26	85.28	84.69
KNN	K = 10, Cosine dist	88.43	87.69	92.48	91.93	89.71	89.08	92.63	88.47	76.08	70.3	88.65	86.19	88.12	87.36	85.26	85.73
DT	Fine, 100 splits	87.22	87.1	91.8	90.11	88.66	87.30	88.11	86.35	91.78	91.36	86.39	85.74	88.65	87.73	85.31	84.74
DT	Medium, 20 splits	87.71	68.98	92.71	92.16	54.78	50.14	88.23	85.94	91.05	91.16	88.61	87.58	89.91	87.82	84.15	84.03
DT	Coarse, 4 splits	67.55	62.83	92.55	92.29	89.35	88.2	77.25	74.03	80.34	80.68	72	70.24	74.23	71.36	68.17	63.6
DNN	10 hidden layers	87.33	85.07	89.67	88.3	91.23	90.95	89.67	87.2	90.28	89.96	89.37	88.09	88.74	88.2	89.91	88.64
EBT	30 learners, 42 k splits	**97.65**	**97.54**	**98.23**	**98.09**	**95.73**	**95.61**	**97.91**	**97.75**	**96.69**	**96.61**	**95.84**	**95.88**	**97.8**	**97.51**	**96.23**	**96.15**

Table 7
Performance investigation of the proposed MSWPT feature extraction vs. other descriptors using the EBT classifier.

| Feature extraction | house 0 | | house 1 | | house 2 | | house 3 | | house 4 | | house 5 | | house 6 | | house 7 | | Time (sec) |
	acc	F1	acc	F1	acc	F1	acc	F1	acc	F1	acc	F1	acc	F1	acc	F1	
Raw data	51.43	46.11	51.97	47.08	49.27	44.66	50.19	46.35	50.81	47.1	49.87	46.42	51.13	47.63	50.8	47.22	/
RMSF	90.74	89.07	92.32	91.19	89.78	88.2	90.92	89.27	90.4	89.77	88.93	88.49	90.15	88.76	89.52	89.04	0.41
MADF	89.32	88.19	90.70	90.22	89.07	87.45	88.93	88.64	89.67	89.14	88.71	86.86	90.27	89.7	89.4	88.56	0.24
WLF	85.16	84.3	85.76	84.79	83.80	83.43	84.87	84.37	83.91	81.58	83.50	82.46	84.07	83.23	83.96	82.67	0.29
ZCF	76.18	75.28	77.23	76.11	73.32	71.37	76.49	76.03	75.41	74.65	73.3	70.98	74.44	73.8	75.81	74.6	0.37
SSC	86.57	86.24	86.90	86.51	84.97	84.39	86.89	86.72	85.51	85.27	83.71	85.94	85.2	85.33	84.65	2.6
ARF	91.25	89.76	91.7	90.28	89.69	89.19	91.28	90.5	90.91	88.73	89.84	89.9	91.77	91.38	90.5	90.29	13.52
DWTF	92.31	90.78	92.84	91.17	91.06	89.85	92.97	91.3	90.46	90.32	91.12	90.71	91.77	90.6	91.09	89.74	0.33
S-Transform	95.34	95.28	96.17	95.49	93.6	93.44	95.25	95.08	94.58	93.97	94.05	93.86	95.85	95.52	93.96	94.12	0.20
MSWPT	**97.65**	**97.54**	**98.23**	**98.09**	**95.73**	**95.61**	**97.91**	**97.75**	**96.69**	**96.61**	**95.84**	**95.88**	**97.8**	**97.51**	**96.23**	**96.15**	0.21

where ε_t is a noise term. The main object of the NILM, is to recover the unknown signals $S_{i,t}$ given only the observed aggregated readings Z_t [78].

On the other hand, the REDD dataset [24] is also used in this framework to mainly compare the performance of the proposed NILM system with state-of-the-art. In this dataset, power consumption fingerprints of six different households are collected at the appliance-level and aggregated circuit. A sampling rate of 3 s has been adopted for a duration of 3–19 days to record consumption data.

4.3. Event detection performance

In this section, we first discuss the selection of the threshold $\tau = 10$ used in the proposed event detection scheme (Algorithm 1). In practice, when Cepstrum coefficients are used, different threshold values can be adopted, e.g. $\tau = 5, 10, 15, 20, 25, 30$. Consequently, selecting the appropriate threshold value is an important step that can affect the event detection performance and further the final performance. To that end, the impact of threshold variation on the event detection performance in terms of the F1 score is assessed in Table 4. It can be noticed that by
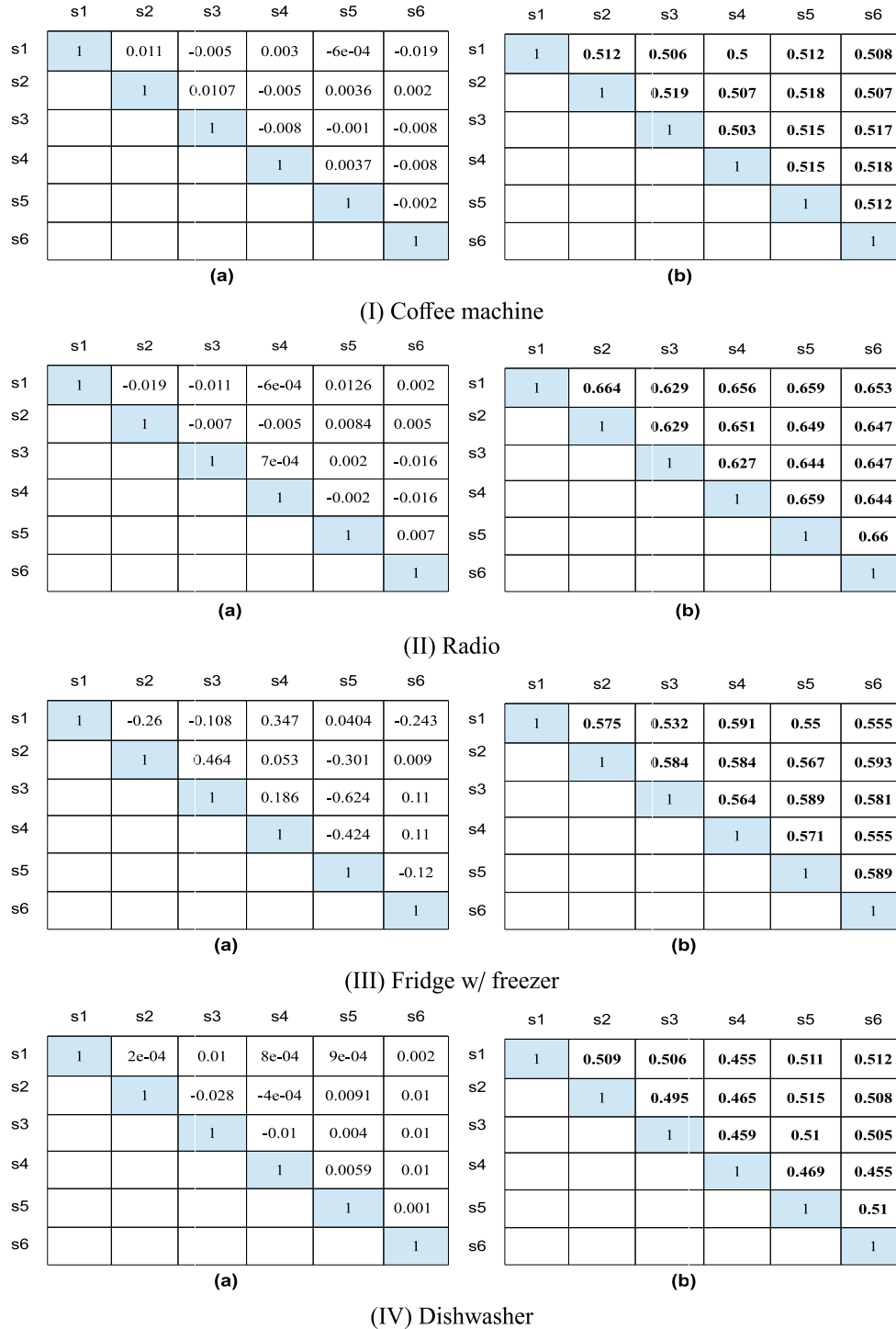
(I) Coffee machine

(a)

	s1	s2	s3	s4	s5	s6
s1	1	0.011	-0.005	0.003	-6e-04	-0.019
s2		1	0.0107	-0.005	0.0036	0.002
s3			1	-0.008	-0.001	-0.008
s4				1	0.0037	-0.008
s5					1	-0.002
s6						1

(b)

	s1	s2	s3	s4	s5	s6
s1	1	0.512	0.506	0.5	0.512	0.508
s2		1	0.519	0.507	0.518	0.507
s3			1	0.503	0.515	0.517
s4				1	0.515	0.518
s5					1	0.512
s6						1

(II) Radio

(a)

	s1	s2	s3	s4	s5	s6
s1	1	-0.019	-0.011	-6e-04	0.0126	0.002
s2		1	-0.007	-0.005	0.0084	0.005
s3			1	7e-04	0.002	-0.016
s4				1	-0.002	-0.016
s5					1	0.007
s6						1

(b)

	s1	s2	s3	s4	s5	s6
s1	1	0.664	0.629	0.656	0.659	0.653
s2		1	0.629	0.651	0.649	0.647
s3			1	0.627	0.644	0.647
s4				1	0.659	0.644
s5					1	0.66
s6						1

(III) Fridge w/ freezer

(a)

	s1	s2	s3	s4	s5	s6
s1	1	-0.26	-0.108	0.347	0.0404	-0.243
s2		1	0.464	0.053	-0.301	0.009
s3			1	0.186	-0.624	0.11
s4				1	-0.424	0.11
s5					1	-0.12
s6						1

(b)

	s1	s2	s3	s4	s5	s6
s1	1	0.575	0.532	0.591	0.55	0.555
s2		1	0.584	0.584	0.567	0.593
s3			1	0.564	0.589	0.581
s4				1	0.571	0.555
s5					1	0.589
s6						1

(IV) Dishwasher

(a)

	s1	s2	s3	s4	s5	s6
s1	1	2e-04	0.01	8e-04	9e-04	0.002
s2		1	-0.028	-4e-04	0.0091	0.01
s3			1	-0.01	0.004	0.01
s4				1	0.0059	0.01
s5					1	0.001
s6						1

(b)

	s1	s2	s3	s4	s5	s6
s1	1	0.509	0.506	0.455	0.511	0.512
s2		1	0.495	0.465	0.515	0.508
s3			1	0.459	0.51	0.505
s4				1	0.469	0.455
s5					1	0.51
s6						1

Fig. 5. Correlation matrices measured between: (a) raw events pertaining to the same appliance classes and (b) their MSWPT features.

increasing the value of threshold, the F1 score performance improves as well until $\tau = 15$ is reached, in which the best performance is achieved. Following, the performance drops as the value of the threshold has increased more than 15. Consequently, $\tau = 15$ was selected as the optimal value and hence used in collecting the results obtained in the rest of this framework.

In order to evaluate the performance of the proposed event detection scheme with state-of-the-art, a comparison is conducted with the chi-squared goodness-of-fit (χ^2 GOF) detector [79] and the Sobel detector [80]. The χ^2 is based on detecting the events through the

assumption that two consecutive timeframes are usually sharing a similar distribution. Following, an x^2 statistic is then performed and a positive detection of an event is occurred if the null hypothesis is rejected. While in [80], the Sobel edge detector is used to detect events in the power signals. In [81], an unsupervised event detector using an on-off pairing and k-nearest neighbors (KNN) model is proposed. In [82], a hybrid event detection approach is introduced, which is based on three main steps defined as: (i) capturing the events using a moving average change with time limit; (ii) adopting a derivative analysis to process devices having long transitions; and (iii) using a filtering process to
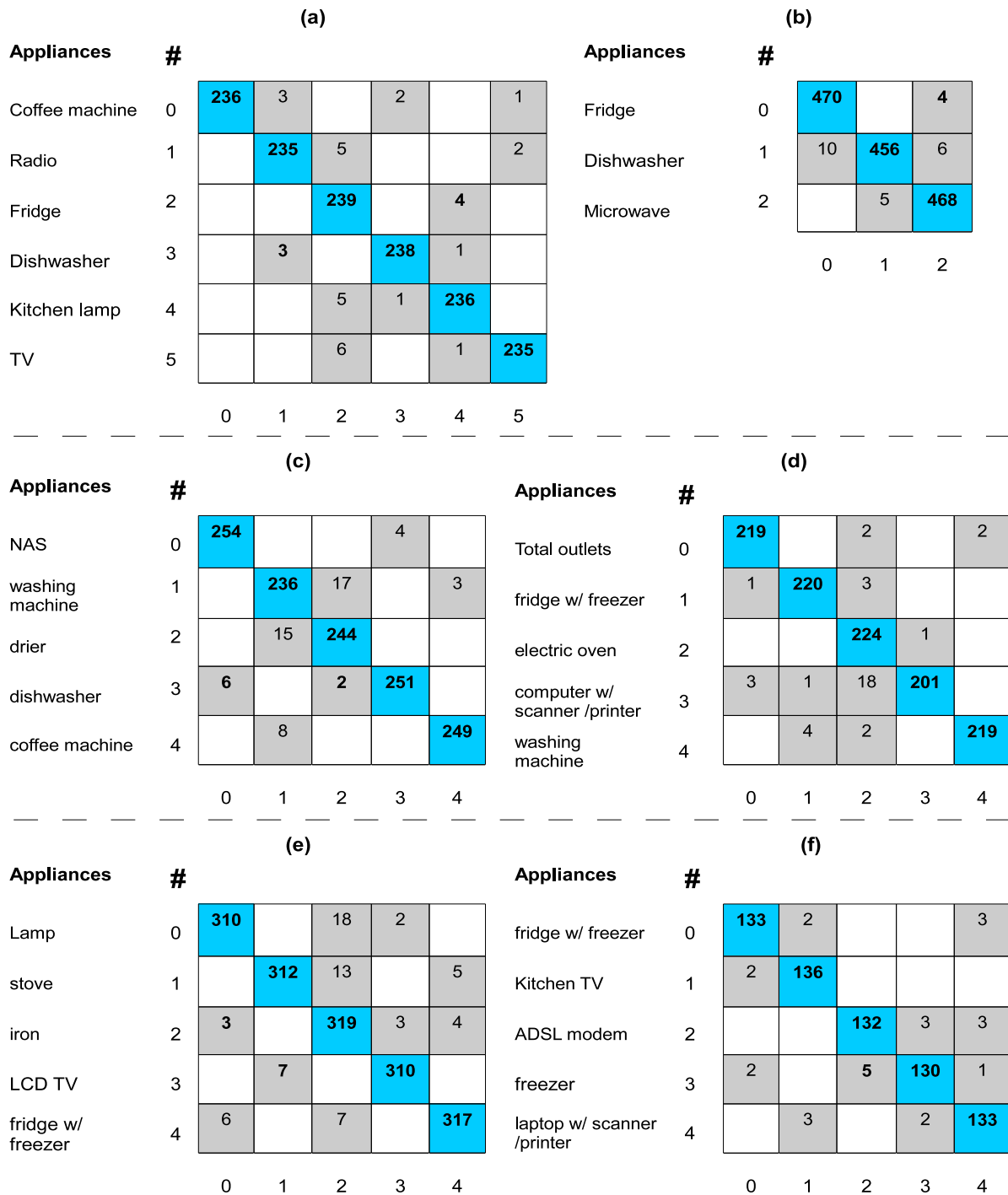
Fig. 6. Example of confusion matrices collected on the GREEND using the proposed NILM system at different households; (a) house 0, (b) house 1, (c) house 2, (d) house 4, (e) house 5 and (f) house 7.

treat devices with a high fluctuation rate.

Through this comparison, for the case of our event detection module and as discussed above, the threshold parameter $\tau = 15$ is adopted to efficiently detect the events. Table 5 presents the average F1 score and time execution results of the proposed event detection scheme compared to the χ^2, Sobel, on-off pairing and hybrid detectors under the GREEND [23] and REDD [24]. These results are collected from the first four houses in each dataset.

It is clearly seen that the proposed Ceptsrum based event detection scheme achieves better performance than χ^2, Sobel and on-off pairing

detectors. Specifically, F1 score rates of 98.93% and 98.01 have been attained on the GREEN and REDD datasets, respectively. Moreover, our event detection scheme has a lower time computation in comparison to the other detectors, in which time executions of 0.37 s and 0.32 s have been reported on the GREEND and REDD datasets, respectively. Moreover, it is worth mentioning that the hybrid detection scheme has a comparable performance with our detector, however it shows the highest time computation, where up to 577.8 s and 572.4 s execution times have been reported under the GREEND and REDD datasets, respectively.

Table 8

Time complexity comparison of the EBT and other machine learning algorithms used in the proposed NILM system.

Algorithms	SVM	KNN	DT	DNN	EBT
Time complexity (with parameter settings)	4.83 s (Linear Kernel) 4.69 s (Quadratic kernel) 5.32 s Gaussian kernel	0.29 s (K = 1, Euclidean dist) 0.28 s (K = 10, W. Euclidean dist) 0.32 s (K = 10, Cosine dist)	0.31 s (Fine, 100 splits) 0.28 s (Medium, 20 splits) 0.3 s (Coarse, 4 splits)	5.67 s (10 hidden layers)	0.33 s (30 learners, 42 k splits)
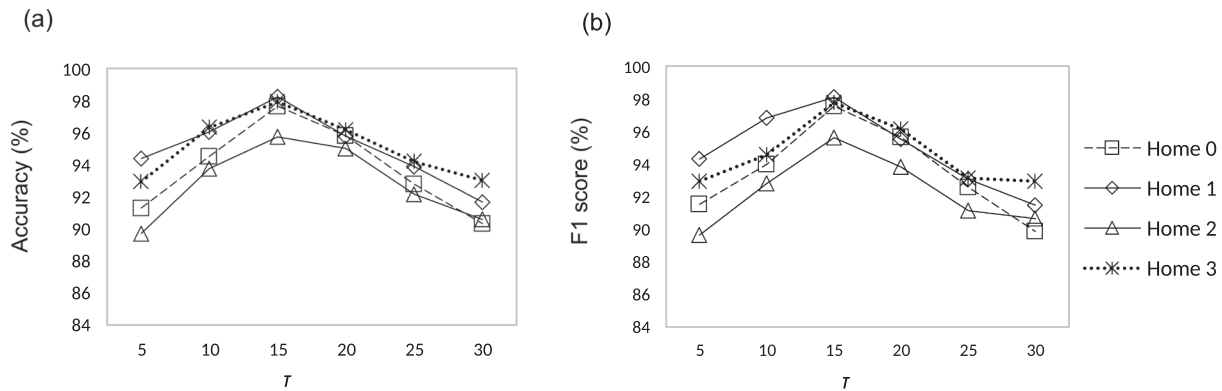
Fig. 7. Impact of varying the event detection threshold τ on the final performance of the proposed NILM system in terms of the: (a) Accuracy and (b) F1 score.

4.4. Investigating machine learning algorithms

After conducting the event detection stage, a vector with a length of 16384 samples is obtained. The latter is then fed to the MSWPT descriptor that results in another vector with 8192 samples. More specifically, when the MSWPT is considered, moving from a level to the next one, the data are split into two parts, one is considered as base frequencies and the second refers to high frequencies. This was possible with the use of low-pass and high-pass filters. The operation is repeated until the desired level ($i = 7$) is reached. Finally, 128 vectors of 128 samples are obtained while 64 of them refer to base frequencies and the other 64 represent high frequencies. The pertinent features are finally extracted by combining the first 64 samples from each vector, in which the pertinent features of each subband are spread. In this context, the final MSWPT feature vector with 8192 samples is constructed.

Through this subsection, the recognition efficiency of the EBT together with various machine learning schemes, including KNN, deep neural network (DNN), SVM, decision tree (DT), is reported in terms of the classification accuracy, F1 score and confusion matrix. As pointed out in Section 3.4, the EBT classifier fuses the classification rates of many separate DT classifiers trained using bagging tree. The classifier parameters are adjusted empirically through varying the number of the weak learners and root splits, and then observing the output performance. Following, the parameters showing the higher accuracy and F1 score rates are finally set as the personalized parameters for this case study. Consequently, in this framework, we combine 30 weak learners using 42 k splits in bagging tree and thus a final robust decision is collected through the combination of these decisions.

Table 6 depicts a comparison between the EBT and the other machine learning algorithms with different classification parameter settings in terms of the accuracy and F1 score.

Overall, it can be witnessed that the EBT scheme has shown promising performances in comparison with the other machine learning algorithms. And by the way, it outperforms all of them in terms of accuracy and F1 score percentages for the six households assessed in this study.

4.5. Comparison with other descriptors

In addition, the proposed MSWPT-based feature extraction is compared to other well-known descriptors, which are based on extracting different kind of power characteristics, including root mean square features (RMSF), absolute deviation features (MADF), zero crossing features (ZCF), waveform length features (WLF), slope sign change features (SSCF), auto-regressive feature (ARF), discrete wavelet transform features (DTWF) [83] and S-Transform. Table 7 depicts the comparison outputs in terms of the accuracy, F1 score and execution time. It can be clearly seen that the proposed MSWPT outperforms the other descriptors on all the households considered in the evaluation in terms of the three evaluation metrics. Furthermore, the S-Transform performs well under all the 8 houses considered in the evaluation, its performance is lower than the MSWPT by an average of 2–3% in terms of the accuracy and F1 score. In terms of time complexity, the MSWPT has the best performance, however the S-transform has almost the same execution time with a very slight difference of 0.01 s.

4.6. Correlation study

To easily comprehend why the proposed feature extraction approach based on MSWPT can achieve good performance for appliance recognition as compared to the other solutions, the normalized correlation between power consumption signals belonging to the same class is explored in this section. To that end, six power consumption signals $s1, s2, ..., s6$ are selected randomly from each class and thereby the correlation coefficients between the various signals are thus measured to illustrate how the MSWPT can help correlate between the signals pertaining to the same class.

Fig. 5 illustrates the NCC matrices estimated between the six raw signals and the respective MSWPT descriptions from four appliance classes, including coffee machine, fridge w/freezer, radio and Dishwasher. As it is shown, the plots at the left side of Fig. 5 portrays the correlation between the original power signals. It can clearly be seen that NCC values are very low and change randomly when comparing
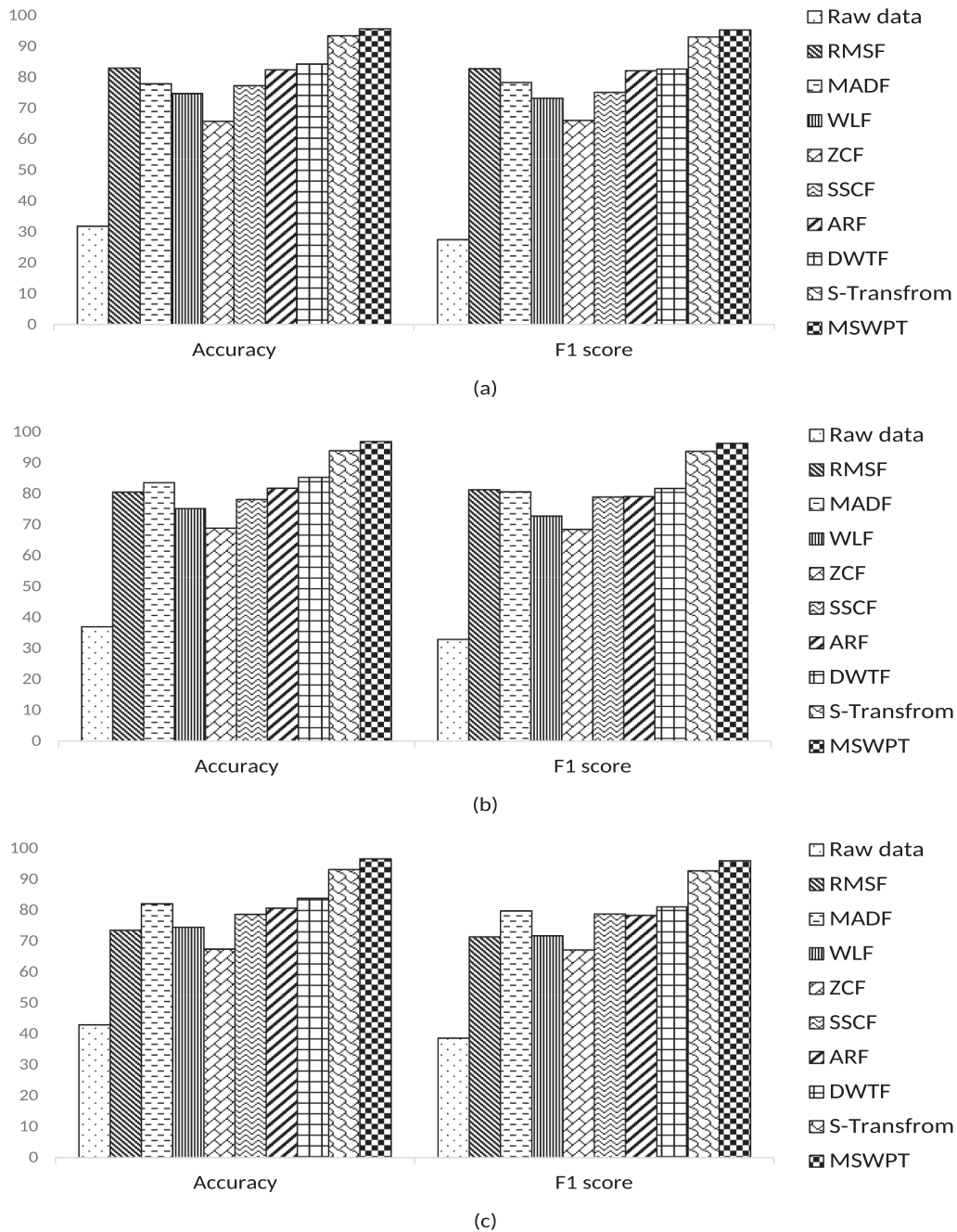
Fig. 8. Accuracy and F1 score performance of the proposed NILM system using the MSWPT feature extraction vs. other descriptors under the REDD dataset: (a) House 0, (b) House 1 and (c) House 2.

two signals, there is no specific interval that can limit NCC measures. This results in a high difficulty to classify raw signals. However, for the case of MSWPT descriptions on the right of Fig. 5, the NCC values clearly outperforms those obtained from the raw power signals. More specifically, NCC values for MSWPT descriptions are more than 0.5, 062, 0.53 and 0.45 for coffee machine, fridge w/freezer, radio and Dishwasher appliance classes, receptively. Therefore, this leads to better results when the MSWPT is adopted because it can increase the correlation between power signals belonging to the same appliance class.

4.7. Confusion matrices

The confusion matrices obtained using the proposed NILM system for six households considered in this study are presented in Fig. 6. For

each particular sub-figure, the performance of the proposed classifier for each appliance class is portrayed. Every unit illustrates the number of samples pertaining to the tag of its corresponding row, which are categorized as can be seen by the tag of its column. The correct classifications are represented by the diagonal units, whereas the other ones reveal the ratio of incorrect classifications. In other words, each unit outward the matrix diagonal exhibits a misclassification. To a large extent, it can be seen that for all of the appliances identified in each household a high percentage of correct classification is achieved using the proposed NILM solution.

4.8. Time complexity

To check the possibility of developing the proposed NILM system as an industrial application in future works, the time complexity of this

Table 9
Performance comparison of the proposed solution with other state-of-the-art approaches under the REDD dataset.

Work	Architecture	Learning scheme	# device classes	Accuracy (%)
[85]	Bayesian Hidden Semi-Markov Models	un-supervised	4	81.5
[86]	Karhunen Loéve	supervised	N/A	87
[32]	HMMs + Iterative k-Means	un-supervised	N/A	85
[76]	AANN	supervised	5	98.7
[58]	CNN + RNN	supervised	20	77.1
Our	MSWPT + EBT	supervised	20	96.36

solution versus the other machine learning based on the MSWPT has also been investigated. In this respect, the algorithms considered in this comparison are implemented using Python 3.7, they have been running on a desktop, having a Core i7-3770S processor, 16 GRAM and 3.1 GHz. Consequently, the obtained complexity results will be closer to the final solution that can be implemented on multi-core embedded platforms such as Jetson Nano, Jetson TX1, Jetson TX2 and ODROID. The power consumption fingerprints collected from house 1 which contains six different appliances are utilized to check the computational complexity. The time complexity of recognition step based on the EBT is compared with the other algorithms through analyzing the power consumption footprints gathered during a period of 10 days. Obtained computational performances in seconds are then presented in Table 8. Henceforth, it can be spotted that the K-NN consumes the lowest complexity, also the EBT has a low time execution that is comparable to the DT. Specifically, the execution time is about 0.33 s, which is less than the sampling rate of data collection. Further, if the system will be implemented on embedded systems with GPU cards the time complexity can be reduced as well. In addition, time computation can also be reduced through re-sampling the collected data to lower sampling rates, e.g. 30 s, 1 min, 2 min, etc.

4.9. Impact of the event detection on the classification performance

In order to investigate the impact of the detection event scheme on the final classification performance, the threshold parameter is varied in a range of 5–30 (τ = 5, 10, 15, 20, 25, 30) and then the accuracy and F1 score performance of the final classification is assessed. Fig. 7 presents an example of the obtained results on home 0, home 1, home 2 and home 3 from the GREEND dataset. It is clearly seen that by varying the threshold values, the accuracy and F1 score are directly affected. Specifically, by increasing the value of the threshold τ, the performance is also increased until τ = 15 is reached, in which the best performance is obtained. However, if the value of the threshold is increased further, the accuracy and F1 score drop significantly.

4.10. Comparison with other descriptors

In order to test the performance of our scheme with other state-of-the-art works, an empirical evaluation is conducted on the REDD dataset [24] that can allow a better comparison since a set of frameworks have been evaluated on it. Aiming at comparing the performance with previous works, we assess the performance the proposed algorithm on three aggregated power signals from three houses, where each household includes a set of electrical appliances. The NILMTK, the open sourced non-intrusive load monitoring toolkit [84], has been used to clean up the null records. Moreover, our models have been trained using the first week of collected footprints from every household for making sure that ON/OFF events of each electrical device are captured at least once.

Fig. 8 illustrates a comparison between the proposed MSWPT based NILM method and other systems built using different descriptors

Table 10
Time complexity of the MSWPT-EBT using the hardware implementation.

Training			Test		
RPI4 Model B	Jetson TX1		RPI4 Model B	Jetson TX1	
	CPU	GPU		CPU	GPU
133.68	45.11	9.37	0.58	0.231	0.039

described previously in Section 4.5. It clearly seen that the proposed MSWPT keeps promising performance under the REDD dataset, in which it outperforms other descriptors. Specifically, accuracy levels of 95.61%, 96.86% and 95.97% are obtained on house 1 (18 devices 620 h), house 2 (9 devices, 258 h) and house 3, respectively. Moreover, it is worth noting that the average performance under the REDD dataset (accuracy = 96.36 %, F1 score = 95.84%) has been slightly dropped in comparison to that obtained on the GREEND dataset (accuracy = 97.87% and F1 score = 97.83%). This can be justified by the fact that the aggregated data used in the REDD dataset are collected directly from the main supply; however, in the GREEND, the aggregated data are gathered through summing the individual appliance footprints. Furthermore, the S-Transform performs well on the REDD dataset, in which their accuracy and F1 score performances are less than those of the MSWPT by 2–3.5%. For example, accuracies values of 93.39%, 93.89%, 93.13% and F1 scores of 92.97%, 93.67% and 92.71% have been achieved on house 1, house2 and house 3, respectively.

4.11. Comparison with existing NILM systems

In addition to investigations executed in the aforementioned sections, a comparative study with other state-of-the-art NILM systems has been conducted in this subsection. To this effect, a comparative analysis is managed in terms of the classification accuracy with reference to the used architecture, number of monitored appliances and the nature learning model (supervised or unsupervised). Table 9 summarizes the comparison outputs. It is clearly seen that the proposed system has better performances than almost techniques considered in this study. Only the performance of the framework proposed in [76] outperforms the performance of our NILM system. However, it is worth noting that the work presented in [76] can only identify 5 appliances, in contrast to our NILM model, in which up to 20 electrical devices are recognized under the REDD dataset.

4.12. Hardware implementation and its time complexity

To clarify the time complexity of our approach via the experiment, we have implemented the MSWPT-EBT on a Raspberry PI 4 (RPI4) model B [87] and Jetson TX1 [88]. The former has a 64-bit quad-core processor and up to 4 GB of RAM, while the latter has an NVIDIA Maxwell graphics processing unit (GPU) with 256 NVIDIA CUDA Cores and 16 GB, hosted on an Ubuntu environment. The overall REDD dataset has been used to evaluate the training and test times.

Table 10 presents the training and test times (in sec) of the proposed NILM system on the RPI4 model B and the Jetson TX1 using multicore central processing unit (CPU) and GPU. It can be clearly seen that PRI4 model has the highest time execution for the training and test procedures, in which the training has been executed in 133.68 s while the test has been achieved in 0.58 s. However, by considering the Jetson TX1 the execution time has been widely reduced, especially when the multicore GPU is used. In this case, the training has been executed in 9.37 s, while the test has been achieved in 0.039 s, i.e. to identify a candidate appliance, only 0.039 s is required on the Jetson TX1 with multicore GPU, which is much lower than the sampling frequency of the REDD datset (1/3 s). This proves that the proposed algorithm can be used for real-time NILM applications.

5. Conclusion

This framework reports a powerful non-intrusive load monitoring system designed based on (1) using a powerful frequency-based technique relying on a Cepstrum filtering to detect appliance events, (2) introducing a novel multi-scale wavelet packet tree descriptor to extract relevant features from detected transition changes, and (3) applying an improved architecture of the ensemble bagging tree to identify electrical devices. The empirical evaluation is conducted on two well-known realistic datasets, namely the GREEND and REDD, which are gathered at 1 Hz and 1/3 Hz, respectively. In addition, an extensive survey of recent non-intrusive load monitoring techniques has been conducted, in which their characteristics, performances and drawbacks are presented.

The proposed non-intrusive load monitoring system accomplishes very satisfying appliance recognition performances in terms of the accuracy, F1 score and computational complexity. Specifically, up to 29 domestic appliances are well identified with an average accuracy of 97.87% in the case of the GREEND dataset. Whereas, up to 96.36% of the accuracy is achieved on the REDD dataset, in which 20 appliance groups are considered in the evaluation study. Consequently, this ascertains the efficiency and applicability of the solution presented over this framework.

A limitation of the proposed NILM system that will be addressed in our future work is mainly the identification of unknown appliances (that do not pertain to any class in the reference dataset). Specifically, because we use a supervised classifier, if an unknown appliance appears it will be affected to one of the classes in the reference dataset. In this context, it will be a false negative detection. To resolve this problem, another identification stage could be deployed to check the similarity of the unknown appliance feature with all the features in the reference dataset and then a threshold parameter can be set to decide whether an appliance effectively belongs to one of the classes in the reference dataset.

Additionally, other challenges still need to be investigated in future works, among others developing an automatic recommendation system for reducing wasted energy based on the use of the proposed non-intrusive load monitoring system, which provides specific appliance consumption rates. Therefore, analyzing those data helps detecting abnormal or anomalous consumption, and hence appropriate recommendations can be generated to promote end-users adopting an energy efficiency behavior.

Declaration of Competing Interest

The authors declare that they have no known competing financial interests or personal relationships that could have appeared to influence the work reported in this paper.

Acknowledgements

References

[1] Alsalemi A, Ramadan M, Bensaali F, Amira A, Sardianos C, Varlamis I, et al. Endorsing domestic energy saving behavior using micro-moment classification. Appl Energy 2019;250:1302–11.

[2] Safarzadeh S, Rasti-Barzoki M. A game theoretic approach for assessing residential energy-efficiency program considering rebound, consumer behavior, and government policies. Appl Energy 2019;233–234:44–61.

[3] Chen VL, Delmas MA, Kaiser WJ, Locke SL. What can we learn from high-frequency appliance-level energy metering? Results from a field experiment. Energy Policy 2015;77:164–75.

[4] Zhou Y, Shi Z, Shi Z, Gao Q, Wu L. Disaggregating power consumption of commercial buildings based on the finite mixture model. Appl Energy 2019;243:35–46.

[5] Cominola A, Giuliani M, Piga D, Castelletti A, Rizzoli A. A hybrid signature-based iterative disaggregation algorithm for non-intrusive load monitoring. Appl Energy 2017;185:331–44.

[6] Haq AU, Jacobsen H-A. Prospects of appliance-level load monitoring in off-the-shelf energy monitors: a technical review. Energies 2018;11(1).

[7] Alsalemi A, Sardianos C, Bensaali F, Varlamis I, Amira A, Dimitrakopoulos G. The role of micro-moments: a survey of habitual behavior change and recommender systems for energy saving. IEEE Syst J 2019;13(3):3376–87.

[8] Liu Y, Wang X, Zhao L, Liu Y. Admittance-based load signature construction for non-intrusive appliance load monitoring. Energy Build 2018;171:209–19.

[9] Nalmpantis C, Vrakas D. Machine learning approaches for non-intrusive load monitoring: from qualitative to quantitative comparation. Artif Intell Rev 2019;52(1):217–43.

[10] Sadeghianpourhamami N, Ruyssinck J, Deschrijver D, Dhaene T, Develder C. Comprehensive feature selection for appliance classification in nilm. Energy Build 2017;151:98–106.

[11] Hosseini SS, Agbossou K, Kelouwani S, Cardenas A. Non-intrusive load monitoring through home energy management systems: a comprehensive review. Renew Sustain Energy Rev 2017;79:1266–74.

[12] Welikala S, Thelasingha N, Akram M, Ekanayake PB, Godaliyadda RI, Ekanayake JB. Implementation of a robust real-time non-intrusive load monitoring solution. Appl Energy 2019;238:1519–29.

[13] Streubel R, Yang B. Identification of electrical appliances via analysis of power consumption. 2012 47th International Universities Power Engineering Conference (UPEC). 2012. p. 1–6.

[14] Alsalemi A, Bensaali F, Amira A, Fetais N, Sardianos C, Varlamis I. Smart energy usage and visualization based on micro-moments. In: Bi Y, Bhatia R, Kapoor S, editors. Intelligent Systems and Applications. Cham: Springer International Publishing; 2020. p. 557–66.

[15] Sardinos C, Varlamis I, Dimitrakopoulos G, Alsalemi A, Bensaali F, Amira A. I want to.... change micro-moment based recommendations can change users. Proc. 8th International Conference on Smart Cities and Green ICT Systems. 2019. p. 1–10.

[16] Seem JE. Using intelligent data analysis to detect abnormal energy consumption in buildings. Energy Build 2007;39(1):52–8.

[17] Spiric JV, Stankovic SS, Docic MB. Identification of suspicious electricity customers. Int J Electr Power Energy Syst 2018;95:635–43.

[18] Araya DB, Grolinger K, ElYamany HF, Capretz MA, Bitsuamlak G. An ensemble learning framework for anomaly detection in building energy consumption. Energy Build 2017;144:191–206.

[19] Yip S-C, Tan W-N, Tan C, Gan M-T, Wong K. An anomaly detection framework for identifying energy theft and defective meters in smart grids. Int J Electr Power Energy Syst 2018;101:189–203.

[20] Wei Y, Xia L, Pan S, Wu J, Zhang X, Han M, et al. Prediction of occupancy level and energy consumption in office building using blind system identification and neural networks. Appl Energy 2019;240:276–94.

[21] Chen Z, Jiang C, Xie L. Building occupancy estimation and detection: a review. Energy Build 2018;169:260–70.

[22] Rashid H, Singh P, Stankovic V, Stankovic L. Can non-intrusive load monitoring be used for identifying an appliances anomalous behaviour? Appl Energy 2019;238:796–805.

[23] Monacchi A, Egarter D, Elmenreich W, D'Alessandro S, Tonello AM. Greend: An energy consumption dataset of households in Italy and austria. 2014 IEEE International Conference on Smart Grid Communications (SmartGridComm). 2014. p. 511–6.

[24] Kolter JZ. Redd: a public data set for energy disaggregation research. In: Proceedings of the 1st KDD Workshop on Data Mining Applications in Sustainability (SustKDD). San Diego, CA, USA: ACM; 2011.

[25] Esa NF, Abdullah MP, Hassan MY. A review disaggregation method in non-intrusive appliance load monitoring. Renew Sustain Energy Rev 2016;66:163–73.

[26] Liu B, Luan W, Yu Y. Dynamic time warping based non-intrusive load transient identification. Appl Energy 2017;195:634–45.

[27] Parson O, Ghosh S, Weal M, Rogers A. An unsupervised training method for non-intrusive appliance load monitoring. Artif Intell 2014;217:1–19.

[28] Basu K, Debusschere V, Douzal-Chouakria A, Bacha S. Time series distance-based methods for non-intrusive load monitoring in residential buildings. Energy Build 2015;96:109–17.

[29] Makonin S, Popowich F, Baji IV, Gill B, Bartram L. Exploiting hmm sparsity to perform online real-time nonintrusive load monitoring. IEEE Trans Smart Grid 2016;7(6):2575–85.

[30] Guedes JDS, Ferreira DD, Barbosa BHG, Duque CA, Cerqueira AS. Non-intrusive appliance load identification based on higher-order statistics. IEEE Latin Am Trans 2015;13:3343–9.

[31] Krull C, Thiel M, Horton G. Testing applicability of virtual stochastic sensors for non-intrusive appliance load monitoring, Electron Notes Theoret Comput Sci 2018;337:119–34 [proceedings of the Ninth International Workshop on the Practical Application of Stochastic Modelling (PASM)].

[32] Kong W, Dong ZY, Ma J, Hill DJ, Zhao J, Luo F. An extensible approach for non-intrusive load disaggregation with smart meter data. IEEE Trans Smart Grid 2018;9(4):3362–72.

[33] Liu Y, Geng G, Gao S, Xu W. Non-intrusive energy use monitoring for a group of electrical appliances. IEEE Trans Smart Grid 2018;9(4):3801–10.

[34] Ji TY, Liu L, Wang TS, Lin WB, Li MS, Wu QH. Non-intrusive load monitoring using additive factorial approximate maximum a posteriori based on iterative fuzzy c-Means. IEEE Trans Smart Grid 2019;10(6):6667–77.

[35] Mengistu MA, Girmay AA, Camarda C, Acquaviva A, Patti E. A cloud-based on-line disaggregation algorithm for home appliance loads. IEEE Trans Smart Grid 2019;10(3):3430–9.

[36] Holweger J, Dorokhova M, Bloch L, Ballif C, Wyrsch N. Unsupervised algorithm for disaggregating low-sampling-rate electricity consumption of households. Sustain Energy Grids Netw 2019;19:100244.

[37] Bonfigli R, Principi E, Fagiani M, Severini M, Squartini S, Piazza F. Non-intrusive load monitoring by using active and reactive power in additive factorial hidden markov models. Appl Energy 2017;208:1590–607.

[38] Cominola A, Giuliani M, Piga D, Castelletti A, Rizzoli A. A hybrid signature-based iterative disaggregation algorithm for non-intrusive load monitoring. Appl Energy 2017;185:331–44.

[39] Henao N, Agbossou K, Kelouwani S, Hosseini SS, Fournier M. Power estimation of multiple two-state loads using a probabilistic non-intrusive approach. Energies 2018;11(1).

[40] Raiker GA, Reddy SB, Umanand L, Yadav A, Shaikh MM. Approach to non-intrusive load monitoring using factorial hidden markov model. 2018 IEEE 13th International Conference on Industrial and Information Systems (ICIIS). 2018. p. 381–6.

[41] Song L, Yao W, Jie T. Non-intrusive load decomposition method based on the factor hidden Markov model. In: 2018 37th Chinese control conference (CCC); 2018. p. 8994–9.

[42] Kong W, Dong ZY, Hill DJ, Luo F, Xu Y. Improving nonintrusive load monitoring efficiency via a hybrid programing method. IEEE Trans Industr Inf 2016;12(6):2148–57.

[43] Mauch L, Yang B. A new approach for supervised power disaggregation by using a deep recurrent lstm network. 2015 IEEE global conference on signal and information processing (GlobalSIP). 2015. p. 63–7.

[44] Chen K, Wang Q, He Z, Chen K, Hu J, He J. Convolutional sequence to sequence non-intrusive load monitoring. J Eng 2018;2018(17):1860–4.

[45] Sirojan T, Phung BT, Ambikairajah E. Deep neural network based energy disaggregation. 2018 IEEE international conference on smart energy grid engineering (SEGE). 2018. p. 73–7.

[46] Baets LD, Ruyssinck J, Develder C, Dhaene T, Deschrijver D. Appliance classification using vi trajectories and convolutional neural networks. Energy Build 2018;158:32–6.

[47] Bonfigli R, Felicetti A, Principi E, Fagiani M, Squartini S, Piazza F. Denoising autoencoders for non-intrusive load monitoring: Improvements and comparative evaluation. Energy Build 2018;158:1461–74.

[48] De Baets L, Dhaene T, Deschrijver D, Develder C, Berges M. VI-based appliance classification using aggregated power consumption data. 2018 IEEE international conference on smart computing (SMARTCOMP). 2018. p. 179–86.

[49] Yang Y, Zhong J, Li W, Gulliver TA, Li S. Semi-supervised multi-label deep learning based non-intrusive load monitoring in smart grids. IEEE Trans Industr Inf 2019:1.

[50] Cui G, Liu B, Luan W, Yu Y. Estimation of target appliance electricity consumption using background filtering. IEEE Trans Smart Grid 2019;10(6):5920–9.

[51] Harell A, Makonin S, Baji IV. Wavenilm: a causal neural network for power disaggregation from the complex power signal. ICASSP 2019–2019 IEEE international conference on acoustics, speech and signal processing (ICASSP). 2019. p. 8335–9.

[52] Xia M, Liu W, Wang K, Zhang X, Xu Y. Non-intrusive load disaggregation based on deep dilated residual network. Electr Power Syst Res 2019;170:277–85.

[53] Zhang Y, Yang G, Ma S. Non-intrusive load monitoring based on convolutional neural network with differential input, Procedia CIRP 2019;83:670–4 [11th CIRP Conference on Industrial Product-Service Systems].

[54] Li Y, Yin B, Wang P, Zhang R. Non-intrusive load monitoring based on convolutional neural network mixed residual unit. J Phys: Conf Ser 2019;1176:022052.

[55] Chen K, Zhang Y, Wang Q, Hu J, Fan H, He J. Scale- and context-aware convolutional non-intrusive load monitoring. IEEE Trans Power Syst 2019:1.

[56] Kong W, Dong ZY, Wang B, Zhao J, Huang J. A practical solution for non-intrusive type ii load monitoring based on deep learning and post-processing. IEEE Trans Smart Grid 2019:1.

[57] Baets LD, Develder C, Dhaene T, Deschrijver D. Detection of unidentified appliances in non-intrusive load monitoring using siamese neural networks. Int J Electr Power Energy Syst 2019;104:645–53.

[58] Murray D, Stankovic L, Stankovic V, Lulic S, Sladojevic S. Transferability of neural network approaches for low-rate energy disaggregation. ICASSP 2019–2019 IEEE international conference on acoustics, speech and signal processing (ICASSP). 2019. p. 8330–4.

[59] He K, Stankovic L, Liao J, Stankovic V. Non-intrusive load disaggregation using graph signal processing. IEEE Trans Smart Grid 2018;9(3):1739–47.

[60] Li D, Dick S. Residential household non-intrusive load monitoring via graph-based multi-label semi-supervised learning. IEEE Trans Smart Grid 2019;10(4):4615–27.

[61] Zhao B, He K, Stankovic L, Stankovic V. Improving event-based non-intrusive load monitoring using graph signal processing. IEEE Access 2018;PP:1.

[62] Lin Y, Tsai M. Development of an improved time-frequency analysis-based nonintrusive load monitor for load demand identification. IEEE Trans Instrum Meas 2014;63(6):1470–83.

[63] Chang H, Lian K, Su Y, Lee W. Power-spectrum-based wavelet transform for non-intrusive demand monitoring and load identification. IEEE Trans Ind Appl 2014;50(3):2081–9.

[64] Gillis JM, Morsi WG. Non-intrusive load monitoring using semi-supervised machine learning and wavelet design. IEEE Trans Smart Grid 2017;8(6):2648–55.

[65] Welikala S, Thelasingha N, Akram M, Ekanayake PB, Godaliyadda RI, Ekanayake JB. Implementation of a robust real-time non-intrusive load monitoring solution. Appl Energy 2019;238:1519–29.

[66] Tabatabaei SM, Dick S, Xu W. Toward non-intrusive load monitoring via multi-label classification. IEEE Trans Smart Grid 2017;8(1):26–40.

[67] Basu K, Debusschere V, Bacha S, Maulik U, Bondyopadhyay S. Nonintrusive load monitoring: a temporal multilabel classification approach. IEEE Trans Industr Inf 2015;11(1):262–70.

[68] Teshome DF, Huang TD, Lian K. Distinctive load feature extraction based on fryzes time-domain power theory. IEEE Power Energy Technol Syst J 2016;3(2):60–70.

[69] Dong M, Meira PCM, Xu W, Chung CY. Non-intrusive signature extraction for major residential loads. IEEE Trans Smart Grid 2013;4(3):1421–30.

[70] Liu C, Akintayo A, Jiang Z, Henze GP, Sarkar S. Multivariate exploration of non-intrusive load monitoring via spatiotemporal pattern network. Appl Energy 2018;211:1106–22.

[71] Chowdhury D, Hasan M. Non-intrusive load monitoring using ensemble empirical mode decomposition and random forest classifier. Digital image & signal processing conference. 2018.

[72] Hasan MM, Chowdhury D, Khan MZR. Non-intrusive load monitoring using current shapelets. Appl Sci 9(24). https://www.mdpi.com/2076-3417/9/24/5363.

[73] Hasan MM, Chowdhury D, Hasan K. Statistical features extraction and performance analysis of supervised classifiers for non-intrusive load monitoring. Eng Lett 2019;27(4).

[74] Jimenez Y, Duarte C, Petit J, Carrillo G. Feature extraction for nonintrusive load monitoring based on s-transform. 2014 Clemson University power systems conference. 2014. p. 1–5.

[75] Rodriguez-Silva A, Makonin S. Universal non-intrusive load monitoring (unilm) using filter pipelines, probabilistic knapsack, and labelled partition maps; 2019. arXiv: 1907.06299.

[76] Morais LR, Castro ARG. Competitive autoassociative neural networks for electrical appliance identification for non-intrusive load monitoring. IEEE Access 2019;7:111746–55.

[77] Breiman L. Bagging predictors. Mach Learn 1996;24(2):123–40.

[78] Batra N, Kukunuri R, Pandey A, Malakar R, Kumar R, Krystalakos O, et al. Towards reproducible state-of-the-art energy disaggregation. In: Proceedings of the 6th ACM international conference on systems for energy-efficient buildings, cities, and transportation, BuildSys '19, New York, NY, USA; 2019. p. 193–202.

[79] Jin Y, Tebekaemi E, Berges M, Soibelman L. A time-frequency approach for event detection in non-intrusive load monitoring. Kadar I, editor. Signal processing, sensor fusion, and target recognition XX, vol. 8050. SPIE: International Society for Optics and Photonics; 2011. p. 697–709.

[80] Czarnek N, Morton K, Collins L, Newell R, Bradbury K. Performance comparison framework for energy disaggregation systems. 2015 IEEE international conference on smart grid communications (SmartGridComm). 2015. p. 446–52.

[81] Yasin A, Khan SA. Unsupervised event detection and on-off pairing approach applied to nilm. 2018 international conference on frontiers of information technology (FIT). 2018. p. 123–8.

[82] Lu M, Li Z. A hybrid event detection approach for non-intrusive load monitoring. IEEE Trans Smart Grid 2020;11(1):528–40. https://doi.org/10.1109/TSG.2019.2924862.

[83] Kahl M, Ul Haq A, Kriechbaumer T, Jacobsen H-A. A comprehensive feature study for appliance recognition on high frequency energy data. In: Proceedings of the eighth international conference on future energy systems, e-energy '17. New York, NY, USA: ACM; 2017. p. 121–31.

[84] Batra N, Kelly J, Parson O, Dutta H, Knottenbelt W, Rogers A, et al. Nilmtk. In: Proceedings of the 5th international conference on Future energy systems - e-energy '14. doi: 10.1145/2602044.2602051.

[85] Johnson MJ, Willsky AS. Bayesian nonparametric hidden semi-markov models. J Mach Learn Res 2013;14(1):673–701.

[86] Dinesh C, Nettasinghe BW, Godaliyadda RI, Ekanayake MPB, Ekanayake J, Wijayakulasooriya JV. Residential appliance identification based on spectral information of low frequency smart meter measurements. IEEE Trans Smart Grid 2016;7(6):2781–92.

[87] Raspberry pi 4 model b. https://www.raspberrypi.org/products/raspberry-pi-4-model-b/ [accessed: 2020-03-04].

[88] Jetson tx1 developer kit. http://www.nvidia.com/object/jetson-TX1-dev-kit.htmll [accessed: 2020-03-04].